

## **Enhanced Absolute and Relative Radiometric Calibration for Digital Aerial Cameras**

**ROBERT E. RYAN, MARY PAGNUTTI, Stennis Space Center, USA**

### **ABSTRACT**

A new laboratory radiometric calibration process has been developed at Intergraph Z/I Imaging and is being implemented for both the DMC and RMK-D camera systems. This new capability enables the development of absolutely radiometrically calibrated products for scientific and remote sensing applications and improves general image color quality and color balance. Although many advanced CCD-based multispectral cameras are capable of being absolutely radiometrically calibrated, their benefits have not been widely exploited by the multispectral aerial remote sensing community. Many quantitative scientific studies incorporating vegetation indices, time series analyses, and change detection require absolute radiometry and atmospheric correction to generate surface reflectance. Dark scenes such as those produced by water and dense vegetation also require atmospheric correction, as atmospheric scatter can easily mask features. Consequently absolute radiometric calibration of aerial digital imagery enhances its utility and improves its ability to be fused with other data sets such as digital elevation data to generate new products. The new laboratory capability enables Z/I Imaging to generate radiometric performance characteristics comparable to those obtained from remote sensing satellite systems. It gives remote sensing scientists a new tool to augment their satellite imagery and is particularly useful in regions of the world that are difficult to acquire with satellite systems because they experience significant cloud cover. This paper discusses absolute and relative radiometry and gives an overview of the new calibration procedure established at Z/I Imaging.

### **1. RADIOMETRY AND REMOTE SENSING**

A new digital camera radiometric calibration laboratory process, traceable to national standards, has been developed at Intergraph Corporation's Z/I Imaging. This new procedure will be implemented for the Z/I Imaging Digital Mapping Camera (DMC) (Heier et al., 2001; Madani, 2004; Neumann, 2003) and the new RMK-D camera system (Intergraph, 2009). The RMK-D is a medium-format camera system with high geometric resolution, 14 bits per pixel radiometric resolution, 70 dB dynamic range, digital forward motion compensation and four-band multi-spectral capability. These calibration procedures, which have been applied to both panchromatic and multispectral camera heads, will not only improve general image color quality and color balance, but will also enable the development of absolutely radiometrically calibrated products for scientific and remote sensing applications.

The newly developed process will enable Z/I Imaging digital aerial cameras to produce radiometrically calibrated imagery with an absolute accuracy comparable to that achievable from both commercial and government satellite remote sensing systems. This level of absolute radiometry will make it possible for Z/I Imaging digital camera users to perform traditional remote sensing tasks that historically were limited to those teams using satellite imagery. It will also allow users of satellite imagery to augment and enhance their projects with aerial digital camera data products.

Multispectral aerial digital imaging systems have traditionally focused on relative radiometric calibrations to cosmetically correct image defects. Typically, image normalization or flat fielding and camera head-to-camera head corrections are used to remove the effects of vignetting and most pixel-to-pixel variations in response. A typical remote sensing industry relative radiometry goal after flat fielding calibration is to have less than 1% variation between pixels (Landsat Data

Continuity Mission (LDCM) Data Specification, 2000). Mosaicking together the large number of aerial frames typically needed to cover a region of interest requires image flat fielding that meets or exceeds this goal. For very uniform scenes, such as dry lake beds, deserts and freshly fallen snow, better than 1% variation after flat fielding may also be required.

Another aspect of radiometry involves the relationship between digital number (DN), brightness (radiance) and integration time, which is typically close to linear over a wide range of signals. In cases where the linearity assumption is justified, data can usually be linearized with a simple transformation. Absolute radiometry transforms DNs into physical radiance and is usually applied after a relative radiometric calibration is performed. Absolute radiometric transformations are directly related to a national laboratory radiance standard. The typical satellite land remote sensing industry absolute radiometry specification is defined such that the difference between the radiance measured by a remote sensing system and that measured by a national standard is less than 5% of the national standard with a performances goal of less than 2% (Landsat Data Continuity Mission (LDCM) Data Specification, 2000).

Absolute radiometry is critical for many scientific remote sensing investigations. It is the foundation to atmospheric correction whereby the atmospheric contribution of a measured signal is separated from that which has been either reflected or emitted from the earth's surface. Many targets of interest, such as water bodies, have relatively small signals as compared to the atmosphere. This phenomenon is illustrated in Figure 1 below. In this example, radiance values are predicted using the Modtran radiative transport code (Berk, 2003) for a mid-latitude summer day at a solar zenith angle of 60 degrees, a visibility of 23 kilometers and a typical rural aerosol. The expected radiance value from a perfectly dark, zero reflectance target is strictly the radiance due to the presence of the atmosphere. Except in spectral regions above 0.65 microns on a vegetated target, the contribution of the atmosphere is a significant if not dominant contributor to the total predicted radiance.

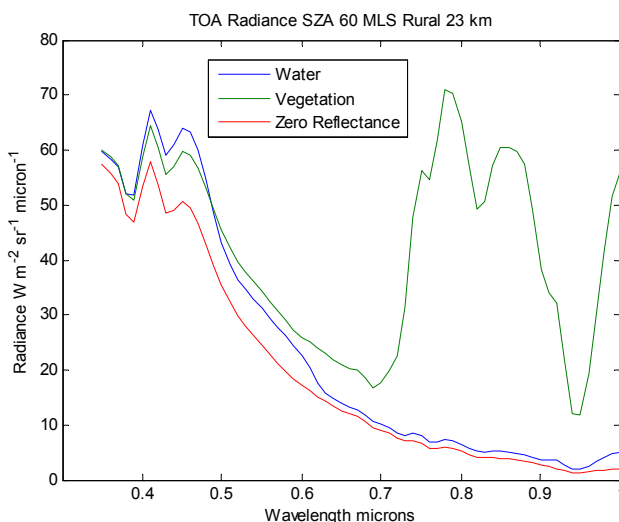


Fig. 1: Predicted radiance of different targets of interest.

Surface reflectance knowledge in the near infrared (NIR) and red bands permits various vegetation indices, such as the Normalized Difference Vegetation Index (NDVI), that are highly correlated with vegetation health, to be calculated (Jensen, 1996). Surface reflectance can also improve classification accuracies and color quality by reducing atmospheric and illumination effects. Techniques that rely on monitoring surface reflectance over time such as time series analyses can also be employed using surface reflectance maps.

Scientists and users of remotely sensed data products are more commonly basing both research conclusions and decision making on results derived from multiple platforms and sensors. These all-source solutions fundamentally require an understanding of both absolute and relative radiometric performance. A critical example of this is the study of climate and climate change. It is impossible to distinguish effects due to varying atmospheric conditions or individual sensor performance from those due to long term

environmental factors without accounting for the atmosphere and tying the data to a standard point of reference.

Absolute radiometry and knowledge of sensor sensitivity performance enables users to optimize their use of digital imaging systems. The high sensitivity characteristics of the DMC and RMK-D cameras for example, enable the cameras to image over an extremely large dynamic range. Knowing the absolute radiometric performance of these camera systems lets users optimize exposure time and spatial resolution to obtain high quality imagery under challenging conditions. The DMC multispectral camera as example has generated reasonably high image quality even while being flown after dusk. The RMK-D camera system also has the potential of extending data collection windows into periods of relatively low light. Light pollution studies and disaster management response activities significantly benefit from an absolute radiometrically calibrated system because it is now possible to both predict and optimize data acquisitions.

The color quality of a digital imaging system is related to its radiometric performance and in general excellent color rendering is easier to achieve when a camera system has stable and repeatable relative and absolute radiometric characteristics. Proper color balancing in fact drives the need for excellent band-to-band relative radiometry. Absolutely radiometrically calibrated imagery together with in-scene knowledge enables atmospheric correction which also enhances the ability to perform color balancing.

### 1.1. Digital Camera Design Properties and Radiometry

Remote sensing, color balancing, pan sharpening and photometry, which relate a digital camera's RGB outputs to human visual response, require a well defined system level spectral response. In general, camera or system level spectral response depends on lens transmission, detector response and filter transmission. The DMC optical system is a telecentric design and is shown in Figure 2. With the exception of the long-wave red channel cut-off, DMC spectral filtering is based on glass absorption filters, which are relatively insensitive to field angle and f-number. The long-wave red channel cut-off, on the other hand, is based on a dielectric stack interference filter design and has a slight sensitivity to both field angle and f-number.

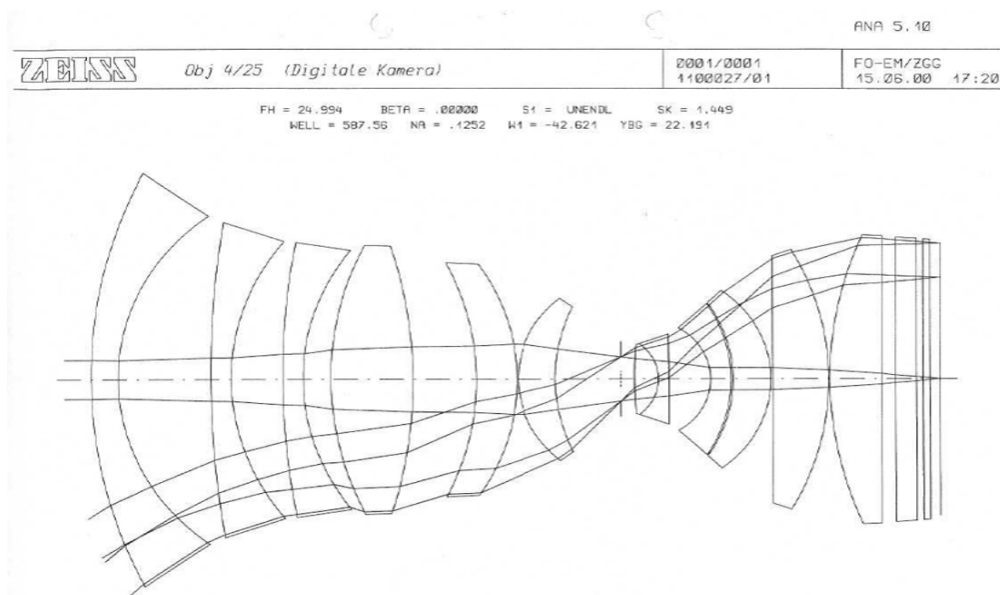


Fig. 2: Optical schematic of multispectral camera showing telecentric design.

The system level spectral response, taken at the Carl Zeiss facility in Jena, Germany, is peak normalized to unity and plotted in Figure 3 below. The system level spectral response is the total estimated response including all optical components and the average CCD detector response. The individual components (lenses, filters and detector) were measured separately and multiplied together to produce the system level response. The Carl Zeiss spectral response characterization process is comparable to the characterization processes performed in the remote sensing community.

The DMC spectral response is similar to that of high resolution satellite systems such as US commercial systems which have been successfully used by the remote sensing community. In comparison, the system level response of the GeoEye IKONOS multispectral satellite sensing system is shown in Figure 4. For both systems, the system level spectral response is dominated by the CCD response and filters. The DMC panchromatic band response, which extends well into the NIR, increases the complexity of pan sharpening but US commercial satellite based multispectral imaging systems (Digital Globe and GeoEye) have similar panchromatic responses and produce excellent results. Because the red channel uses interference filters, it has increased sensitivity to different f-number settings.

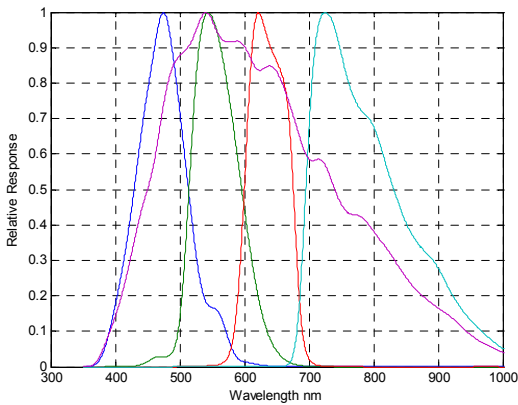


Fig. 3: DMC system level spectral response.

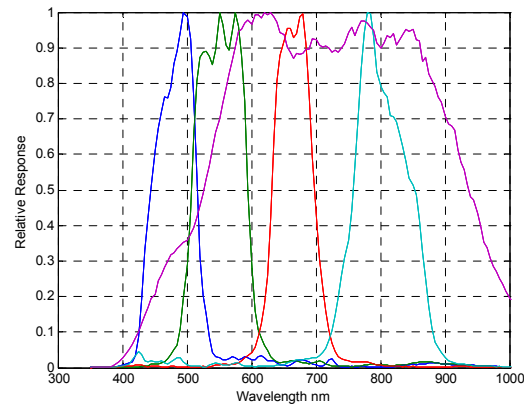


Fig. 4: IKONOS system level spectral response.

The peak wavelength, 50% points and 10% points provide quick values to describe the system level spectral response and are shown for both the DMC and IKONOS sensors in Table 1.

Table 1: DMC and IKONOS Peak, 50% and 10% Spectral Response Values.

| Band  | DMC       |                 |                 | IKONOS    |                 |                 |
|-------|-----------|-----------------|-----------------|-----------|-----------------|-----------------|
|       | Peak (nm) | 50% Points (nm) | 10% Points (nm) | Peak (nm) | 50% Points (nm) | 10% Points (nm) |
| Blue  | 475       | 429-514         | 319-579         | 495       | 445-516         | 426-534         |
| Green | 545       | 514-600         | 497-635         | 550       | 506-595         | 489-611         |
| Red   | 620       | 600-676         | 584-690         | 680       | 632-698         | 611-721         |
| NIR   | 725       | 695-831         | 681-968         | 780       | 757-853         | 724-882         |
| Pan   | 540       | 450-739         | 392-944         | 620       | 526-937         | 475-1031        |



Fig. 5: DMC installed on an aircraft.

Even though there are many similarities to satellite remote sensing systems, aerial digital cameras are designed and flown under vastly different and challenging environmental conditions. To start, the systems must be designed to withstand the forces associated with multiple take-off and landings. Aircraft operate under various atmospheric and turbulent conditions which place vibration, temperature and pressure loads on the digital camera and the systems are also exposed to dirt, sand, dust and moisture. The extremely rugged design of Z/I cameras, one of which is shown installed on an aircraft in Figure 5, aims to maintain their performance under the harshest conditions.

## 2. LABORATORY RADIOMETRIC CALIBRATION

Absolute and relative radiometric calibration can be achieved in the laboratory prior to in-flight operation and are discussed below.

### 2.1. Theory

The DN value associated with a given pixel after dark pixel subtraction is performed depends on the in radiance, spectral response, detector size, solid angle subtended by the lens system aperture and integration time and can be evaluated with expressions similar to the one provided below:

$$DN = G A_d \Omega \tau \int_0^{\infty} L(\lambda) S(\lambda) d\lambda$$

Where:

- $DN$  = Digital number [counts]
- $L$  = Spectral radiance [ $W/(cm^2 \text{ sr nm})$ ]
- $S$  = System level spectral response [(electrons/s)/W]
- $\lambda$  = Wavelength [nm]
- $G$  = Gain coefficient [counts/electrons]
- $A_d$  = Area of detector [ $cm^2$ ]
- $\Omega$  = Lens solid angle [sr]
- $\tau$  = Integration or exposure time [s]

This expression can be simplified and used to define the dependencies for converting calibration. The first simplification is to work in average spectral radiance. The average spectral response can be written as indicated below (Schott, 2007). The advantage of this form is that only the shape of the system level spectral response is needed since the exact magnitude and units cancel after division.

$$\bar{L} = \frac{\int_0^{\infty} L(\lambda) S(\lambda) d\lambda}{\int_0^{\infty} S(\lambda) d\lambda}$$

Where:

$\bar{L}$  = Average spectral radiance [W/(cm<sup>2</sup> sr nm)]

For a linear system such as a CCD system that has had dark frame data subtracted, the average spectral radiance can be related to the DN value associated with a pixel by:

$$\bar{L} = K DN$$

Where:

$K$  = calibration coefficient [(W/(cm<sup>2</sup> sr nm))/counts]

For many satellite based systems, the absolute radiometric calibration coefficient is a single number since the f-number and integration time is fixed. For aerial digital cameras, however, both the f-number and integration time can be selected.

Noting that the solid angle  $\Omega$  is inversely proportional to the square of the f-number we can write:

$$\bar{L} = K' \frac{\tau}{f_{number}^2} DN$$

Where:

$K'$  = calibration coefficient [(W/(cm<sup>2</sup> sr nm s))/counts]

$f_{number}$  = f-number

## 2.2. Implementation

To enable laboratory-based relative and absolute radiometric measurements, a new laboratory radiometric calibration apparatus was designed and constructed and is shown in Figure 6 below. It consists of a 51 cm (20 inch) diameter integrating sphere, with a 15 cm diameter exit aperture, xenon arc and tungsten source lamps, power supplies, spectrometer, computer interface, custom camera mount, and electronics to drive the digital camera.

In this laboratory set-up, the digital camera module to be measured is mounted over the integrating sphere and lowered slightly below the exit aperture of the sphere. Measurements are taken of the extremely uniform light field generated within the integrating sphere at specific f-numbers and exposure settings.

The spectral distribution of the light source is generated by combining xenon arc and tungsten light sources, controlled with variable apertures, which are uniformly mixed within the sphere. The brightness of the light field is monitored using a calibrated US National Institute of Standards (NIST) traceable spectrometer. The resulting combined source spectrum more closely represents a solar spectrum than traditional single sources based on tungsten lamps as shown in Figure 7 below. The integrating sphere radiance level design goal was to exceed the top-of-the-atmosphere (TOA) spectral radiance distribution associated with a 25% reflective target for a 60 degree solar zenith angle clear day.

The integrating sphere's spectral radiance is calibrated. Over the 400-1000 nm spectral range the expected absolute radiometric accuracy of the integrating sphere is less than 1% difference from a national standard.

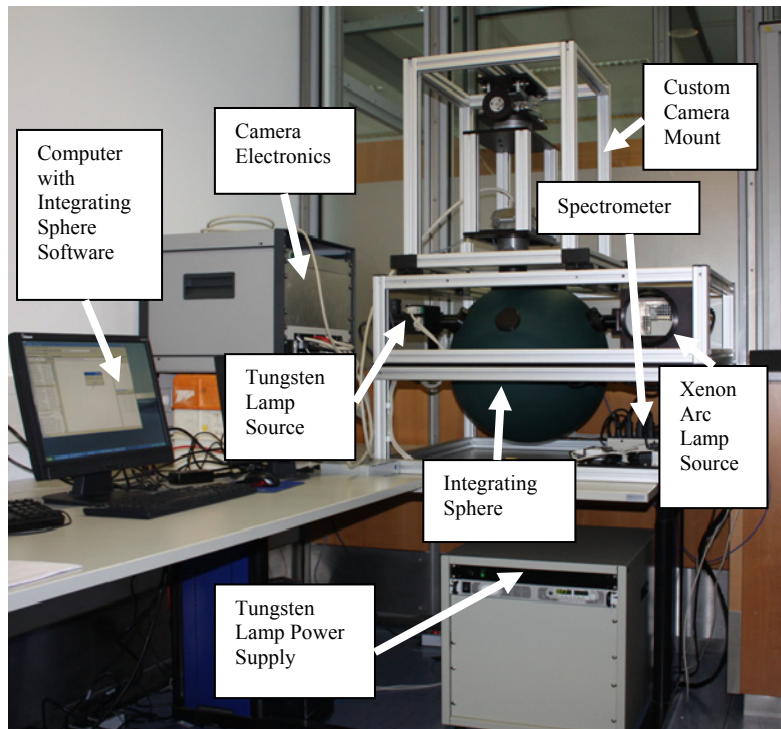


Fig. 6: Laboratory radiometric calibration set-up.

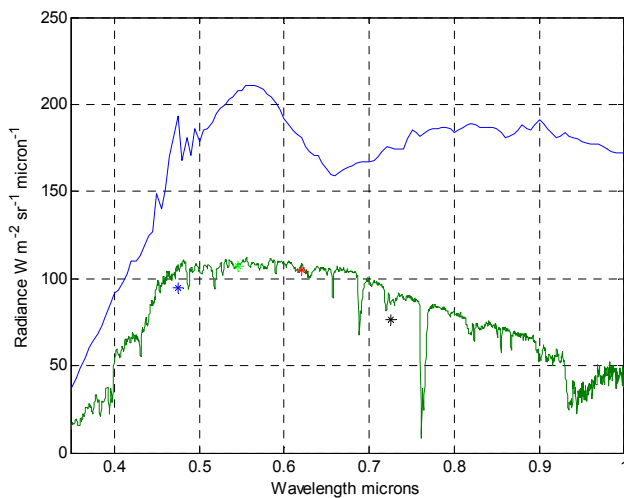


Fig. 7: Sample integrating source spectra and design goal correspond to target goals for blue, green, red and NIR bands.

The radiometric calibration sphere and spectrometer are operated through a graphical user interface (GUI) written using the MATLAB® vector-based scientific programming language. The custom software interfaces with several hardware dynamic link libraries (DLLs) to provide a single user interface to the lamp power supplies, variable apertures and spectrometer.

Relative and absolute radiometric calibrations are achievable using this laboratory set-up coupled with custom calibration algorithms also written in MATLAB, which has a large library of mathematical and image processing functions. The new radiometric

calibration procedures correct for vignetting by performing flat field corrections as shown in Figure 8 below. In this example, the DMC multispectral NIR camera head measured the light field within the integrating sphere. The acquired image is shown in the upper left corner of the figure. The corresponding pixel values are plotted as a 3-D mesh plot in the upper right corner of the figure. The mesh plot clearly shows a hot spot in the center of the image along with expected off-axis roll-off. The lower portion of the figure shows the corrected image and corresponding mesh plot that exhibits the expected increase in gain off-axis.

Linearity measurements are made by changing the exposure time and/or integrating sphere radiance level.

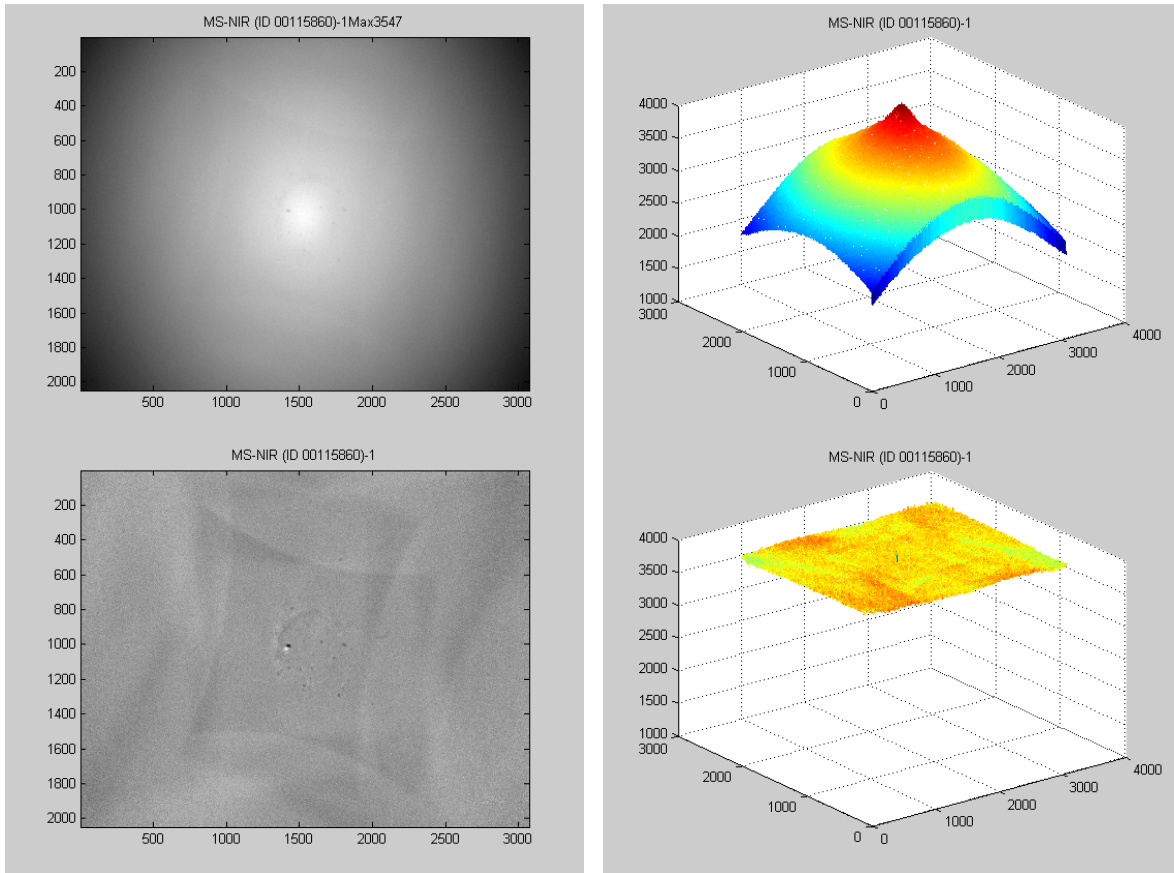


Fig. 8: Example flat fielding.

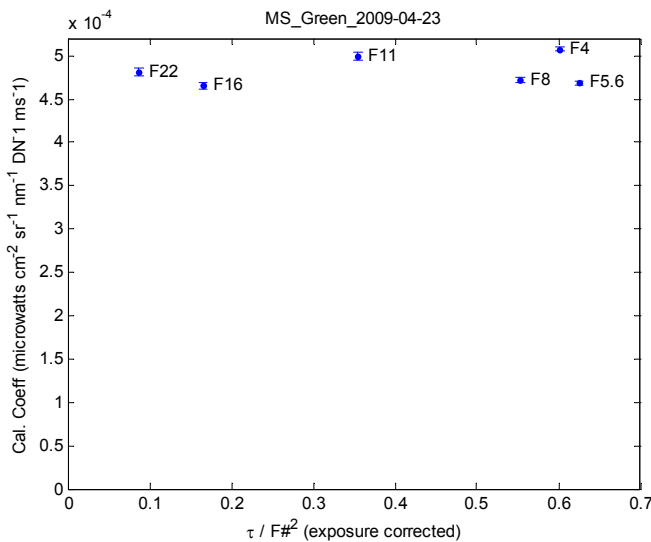


Fig. 9: Radiometric calibration dependency on exposure and aperture.

This measurement apparatus can also perform absolute radiometric calibrations, the results of which are shown in Figure 9. In this example, calibration coefficients were calculated for the DMC multispectral green camera module for six different f-numbers: f-4, f-5.6, f-8, f-11, f-16 and f-22. Each f-number calibration was performed at a specific exposure time and integrating sphere radiance level to achieve high signal-to-noise imagery. Measurement uncertainties are noted as vertical lines in the figure. These resulting calibration coefficients can be multiplied by image DN values to obtain engineering units of radiance after correcting for f-number and integration time. Although

the calibration coefficients are relatively consistent between f-number settings, each f-number requires a specific calibration factor. There is a about a 5% variation in calibration coefficients over

the range of f-numbers measured, which if not accounted for, would exceed the 5% or better radiometric accuracy goal.

Although a comprehensive uncertainty analysis is currently in development, preliminary measurements and some analysis allow us to provide an initial estimate of the performance of the calibration system. The uncertainty in the absolute radiometric calibration coefficient can be written as:

$$\frac{\sigma_{K'}}{K'} = \sqrt{\left(\frac{\sigma_L}{L}\right)^2 + \left(\frac{2\sigma_{fnumber}}{fnumber}\right)^2 + \left(\frac{\sigma_{DN}}{DN}\right)^2 + \left(\frac{\sigma_\tau}{\tau}\right)^2}$$

Where:

$\sigma$  = Uncertainty of a parameter

The uncertainty equation in practice is simplified by combining terms. For example any uncertainty in exposure time will be reflected in uncertainty in DN. Following the newly established radiometric procedures and taking into account the uncertainties of each parameter in the above equation, the radiometric accuracy of the DMC can be expected to be approximately 3% in the laboratory. The RMK-D has been designed to provide improved f-number and integration time knowledge thereby reducing DN variations and should provide improved absolute radiometric accuracy.

### 3. IN-FLIGHT RADIOMETRIC CALIBRATION

Radiometric calibration should be validated in flight to insure that the harsh operating conditions do not adversely affect results. In-flight calibration can also be used to identify and monitor any temporal effects such as drift. For this type of work, reflectance targets, sun photometers and radiative transfer codes are used to estimate the at-sensor radiance and used to validate or update radiometric calibrations. Unlike satellite imagery the at-sensor aerial digital camera radiance levels will have some altitude dependence. To simplify the radiative transfer calculations the sensor can be flown above the aerosol boundary layer, which is typically less than 2 kilometers during calibration test flights. The radiative transfer above this layer is relatively constant and can be modeled. For lower flight altitudes or in cases where the aerosol boundary layer is higher, additional measures have to provide boundary conditions for radiative transfer modeling. The excellent thermal stability of the Z/I Imaging systems will allow the DMC and RMK-D camera systems to be flown at high altitudes simplifying the radiative transfer calculations.

### 4. CONCLUSIONS AND OUTLOOK

In summary, Z/I Imaging has developed a radiometric calibration procedure to perform both relative and absolute radiometric measurements. This procedure can be applied to both the DMC and RMK-D camera systems. This assessment yields radiometric performance characteristics comparable to that obtained with remote sensing satellite systems and positions Z/I Imaging to successfully compete in this market. This capability gives remote sensing scientists a new tool to augment their satellite imagery and is particularly useful in regions of the world that experience significant cloud cover, such as the equator. It is also highly useful for those applications that require imagery collected repeatedly at times much faster than that achievable with single satellites.

## 5. ACKNOWLEDGEMENTS

The authors would like to thank the Z/I Imaging team in Aalen Germany for their technical comments, guidance and discussions, their careful data collection and ancillary information gathering required to collaborate and develop this calibration process. In addition, the authors thank the staff at Innovative Imaging and Research for developing software, analyzing data and providing technical support.

## 6. REFERENCES

- Berk, A., G. P. Anderson, P. K. Acharya, M. L. Hoke, J. H. Chetwynd, L. S. Bernstein, E. P. Shettle, M. W. Matthew & S. M. Adler-Golden (2003): MODTRAN4 Version 3 Revision 1 User's Manual. Air Force Research Laboratory, Space Vehicles Directorate, Air Force Material Command, Hanscom AFB, MA USA.
- Heier H., C. Dörstel & A. Hinz (2001): DMC – The Digital Sensor technology of Z/I Imaging, Photogrammetric Week 2001, Eds. D. Fritsch / R. Spiller, Wichmann, Heidelberg pp. 93-103.
- Intergraph RMK-D Camera System Product Sheet, (2009).
- Jensen, J. (1996): Introductory Digital Image Processing. NJ: Prentice-Hall.
- Landsat Data Continuity Mission (LDCM) Data Specification, (2000).
- Madani, M., C. Heipke, C. Dörstel & K. Jacobsen (2004): DMC Practical Experience and Accuracy Assessment, ISPRS Congress Istanbul 2004, International Archive of the ISPRS.
- Neumann, K. (2003): Aerial Mapping Cameras – Digital versus Film. The benefits of a new technology. Proceeding from the ASPRS 2003 conference, May 5 - 9, 2003.
- Schott, J. (2007): Remote Sensing: The Image Chain Approach, USA: Oxford University Press.